TECHNICAL SCIENCES
Abbrev.: Techn. Sc., No 15(2), Y 2012

A COMPARISON BETWEEN CONTACT AND TAPPING AFM MODE IN SURFACE MORPHOLOGY STUDIES

***Mirosław Bramowicz*[1], *Sławomir Kulesza*[2], *Kazimierz Rychlik*[3]**

[1] Chair of Materials and Machinery Technology
[2] Chair of Relativistic Physics
[1, 2] University of Warmia and Mazury in Olsztyn
[3] Institute of Mechanised Construction and Rock Mining, Warszawa

K e y w o r d s: atomic force microscopy, AFM, surface topography.

A b s t r a c t

The paper presents recent results from studies of a surface topography of a platinum calibration grid on silicon substrate obtained in both contact and tapping modes of the AFM microscope. The results are analyzed in order to determine the influence of the scan set-up and the SPM probe onto estimated fractal parameters and surface anisotropy ratio.

Introduction

Atomic Force Microscopy (AFM) makes use of the forces between two bodies placed very close to each other (from few nanometers up to tens of nanometers). Such forces result from either atomic or particle interaction at a very small distance. Typically, one of the interacting bodies is a sharp tip mounted on an elastic cantilever, whereas the other is the surface under study (see Fig. 1).

When the tip is approaching the surface, the force appears at a certain point. However, both the magnitude of the force, as well as its character (attractive, repulsive) changes with the tip-surface distance, as it is shown in Figure 2.

In the beginning, the tip-surface interaction is dominated by long-range, attractive forces, for example, magnetic ones. When the tip comes closer to the surface, it is attracted much larger due to electrostatic van der Waals forces of the order of 10^{-12} N. Below 1 nm, however, the tip becomes repelled by the

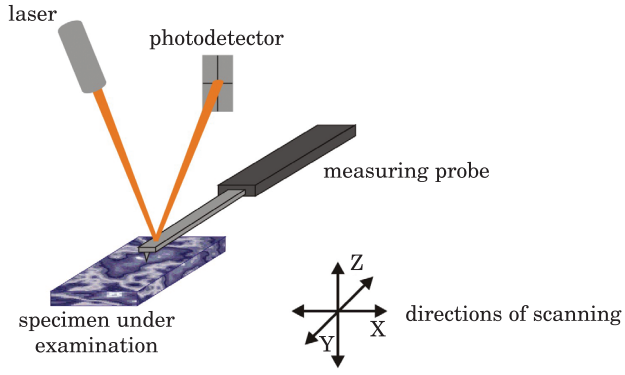

Fig. 1. Schematic description of the AFM principle
Source: MIRONOV 2004.

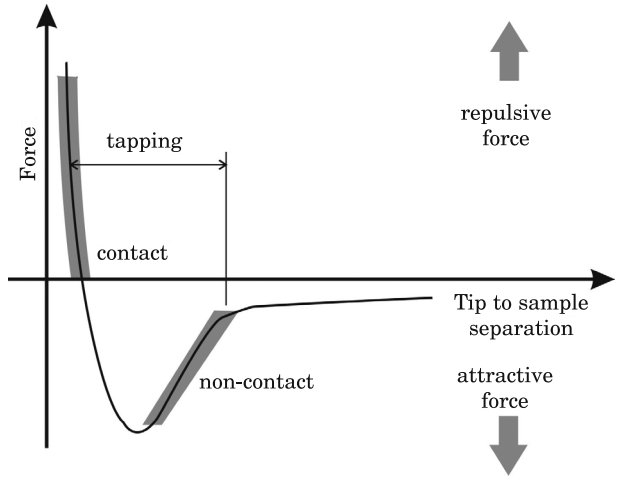

Fig. 2. Forces between the AFM tip and a scanned surface
Source: MIRONOV 2004.

surface as a result of overlapping electron clouds (Pauli exclusion principle). Repulsive forces are of the order of 10^{-9} N, which can be used to adjust the optimal tip-surface distance in the contact and tapping modes (SAINT JEAN et al. 1999). Mutual tip-surface interaction is usually described by the Lennard-Jones potential $U_{L\text{-}J}$:

$$U_{L\text{-}J}(r) = U_0 \left\{ -2\left(\frac{r_0}{r}\right)^6 + \left(\frac{r_0}{r}\right)^{12} \right\} \tag{1}$$

where:
r is the tip-surface distance, r_0 – the tip-surface distance at which the potential reaches its minimum, whereas U_0 – the minimal value of the potential. The first term in Equation (1) corresponds to long-range attractive forces due to dipole interaction, while the second one – corresponds to short-range repulsive forces due to overlapping electron clouds (MIRONOV 2004).

When working in the contact mode, the tip (or the surface, depending on the construction details) is moved along *XY* plane, and the cantilever deflection detected by the 4-section photodiode reflects the surface topography (HOWLAND, BENATAR 2002, BRAMOWICZ, KLYSZ 2007). On the other hand, in the tapping mode the cantilever is additionally forced to oscillate in a vertical direction, at a frequency close to its resonant frequency, and the photodiode measures the amplitude of the oscillation. Despite being used for similar purposes, each scanning mode gives insight into different aspects of the tip-surface interactions (Fig. 2). Contact mode actually relies on the repulsive force solely, while the tapping mode exhibits a large variety of forces, not only repulsive, but also attractive ones.

Experimental procedure

AFM measurements described below concern the effect of the scanning mode on the quality of obtained 3-dimensional surface images and the statistical parameters of the surface topography. Several measurements were carried out using platinum calibration grid (PG) as the reference (grating made from platinum sputtered onto silicon substrate with 1 μm period and 100 nm step height from Bruker). Multimode 8 system (Bruker) allowed for AFM imaging in both contact as well as tapping modes making use of the ScanAsyst-Air SPM probes (the tip radius 2 nm and the cantilever spring constant 0.4 N/m). Each surface profile was sampled at 512 equidistant points, each image was composed of 512 lines. The scan size varied between 0.5 and 50 μm, while the aspect ratio uqual to 1 (square scan area). AFM measurements resulted in 2-dimensional square matrices storing data on local surface heights above a reference level.

In order to characterize the surface topography and to compare the results obtained in the contact and tapping modes, the following statistical parameters were used:
– Root-mean-square deviation of the surface S_q (according to PN-EN ISO 25178-6):

$$S_q = \sqrt{\frac{1}{MN}\sum_{k=0}^{M-1}\sum_{l=0}^{N-1}[z(x_k, y_l)]^2} \tag{2}$$

– Anisotropy coefficient S_{tr} defined as the ratio between the correlation lengths τ of the normalized autocorrelation function $R(\tau,\theta)$ measured along its fastest and slowest decay from the maximum value (1.0) down to 0,2 (MAINSAH et al. 2001):

$$0 < S_{tr} = \frac{\mathrm{Min}\{\tau : R(\tau,\theta) \to 0{,}2\}}{\mathrm{Max}\{\tau : R(\tau,\theta) \to 0{,}2\}} \leq 1 \tag{3}$$

– Fractal dimension D and topothesis K determined using the structure function $S(\tau)$ (MAINSAH et al. 2001):

$$S(\tau) = \langle[z(x) - z(x + \tau)]^2\rangle \tag{4}$$

where:
$\langle\ \rangle$ stands for the average.

On a log-log scale, the structure function $S(\tau)$ draws a characteristic curve that can be approximated by two straight lines: the one inclined at an certain angle for small τ values, and the other which is almost flat for large τ values. The structure function $S(\tau)$ obeys the power law within the small τ range according to (MAINSAH et al. 2001):

$$S(\tau) = K\tau^{2H} \tag{5}$$

where:

$$K = \frac{\pi G^{2(D-1)}}{2\Gamma(5 - 2D)\sin[(2 - D)\pi]} \tag{6}$$

where:
G is the scale factor, Γ is the Euler function, whereas $H = 2 - D$ is the Hurst parameter (HARTMANN 1997, MAINSAH et al. 2001).

Results

Topography maps recorded in contact mode accompanied by the spectra of the area autocorrelation function are shown in Figure 3, and similar data measured in the tapping mode are shown in Figure 4. At first glance, contact mode provides better image contrast, whereas tapping mode exhibits on the scanned surface tiny particles with the mean height not exceeding 10 nm. Such a result is probably due to surface inhomogeneities detected by vibrating probe, because any disturbance to the tip-surface interaction (localized adhesion force, for example) gives rise to huge oscillation frequency shift when working close to the resonant frequency. On that account the tapping mode is far more sensitive to any surface inhomogeneity than the contact mode being, however, less destructive to a sample surface.

By analyzing the spectra of the autocorrelation function for the scan size 0.5 and 1.0 μm shown in Figure 3 and Figure 4, the surface anisotropy can be seen. Indeed, the images exhibit spectra with only one central peak, elongated along the axis of surface anisotropy. On the contrary, when the scan size increases above 5 μm, the spectra of the autocorrelation function become isotropic, although highly periodic.

Figure 5 exhibits significant similarity between both imaging modes in terms of the surface roughness S_q as long as the scan size exceeds 5 μm. For smaller scan areas, however, S_q is noticeably higher in contact mode with respect to tapping mode even though the latter is more sensitive to surface inhomogeneities that should result in larger roughness, as it was mentioned previously. Unfortunately, no reason has been given so far to explain observed discrepancy.

Analysis of 2-dimensional spectra of the autocorrelation functions along the main axes of anisotropy (a1 and a2) for the scan size 0,5 and 1 mm, and along the x and y directions for the scan size 5, 10, 20 and 50 mm, allowed for determination of the anisotropy coefficient S_{tr} according to Eq. (3). The plot of S_{tr} vs. scan size is shown in Figure 6.

Figure 6 shows that independent of the scanning mode, S_{tr} values rise asymptotically to a value close to 1 when the scan size is larger than 5 μm. Small deviation from the unity is probably due to the tip asymmetry as the tip shape convolves with the topography, but this effect is not concerned here. What is important, S_q approaches asymptotical value when the scan size exceeds the grid period. On the other hand, for the scan size equal to 0,5 and 1 μm, S_{tr} values significantly decrease, because the scan size does not cover a single pattern cell. In such a case, anisotropy ratio strongly depends on the scan size. Similar observations were reported previously (BRAMOWICZ 2009) from studies of the anisotropy coefficient of the microstructure of martensitic steel in Ni-Mn-Ga alloys.

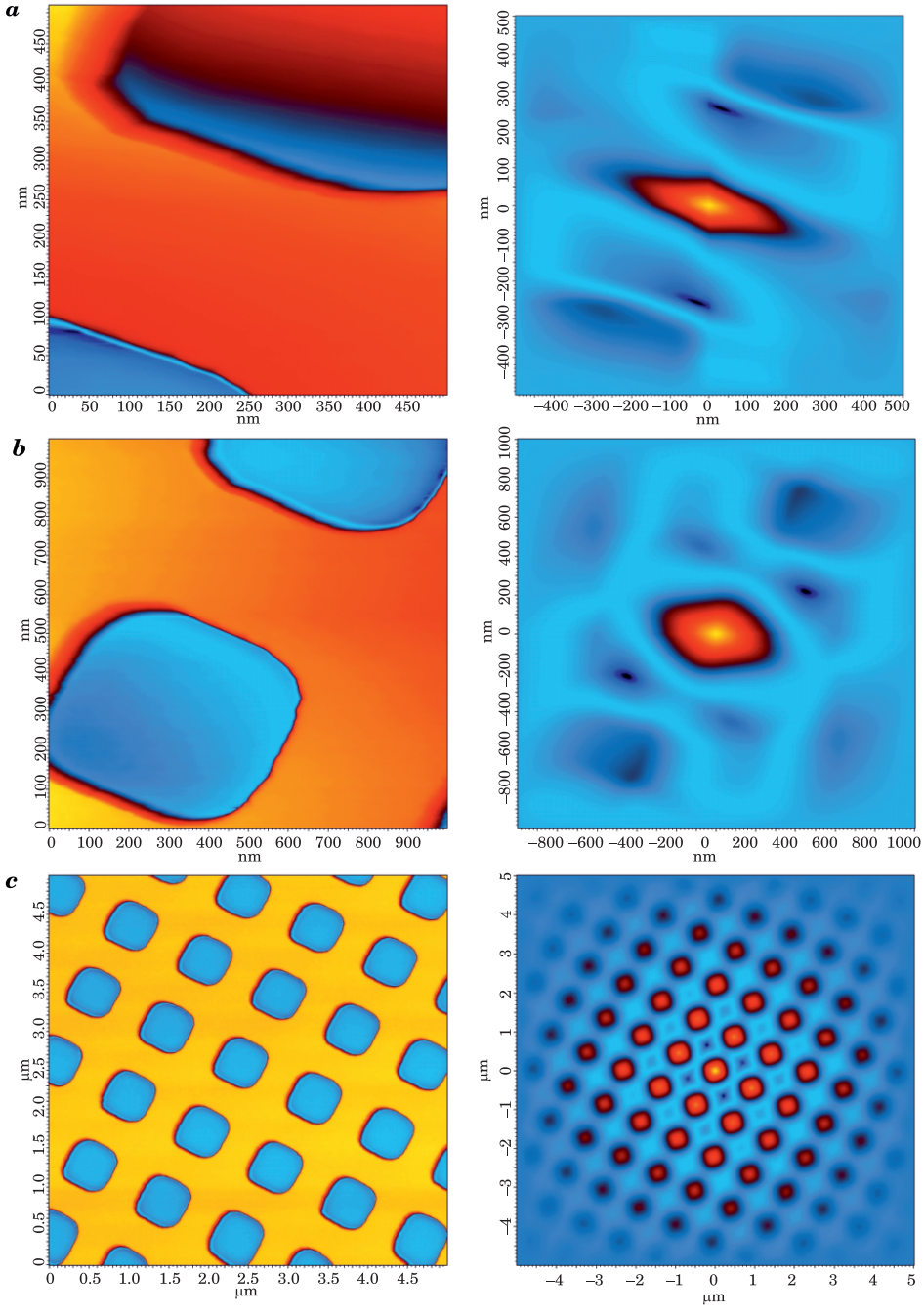

Fig. 3. Surface topography (left) and the spectra of the surface autocorrelation function (right) of the reference PG sample in the contact mode. Scan size, respectively: *a* – 0,5×0,5 μm, *b* – 1×1 μm, *c* – 5×5 μm

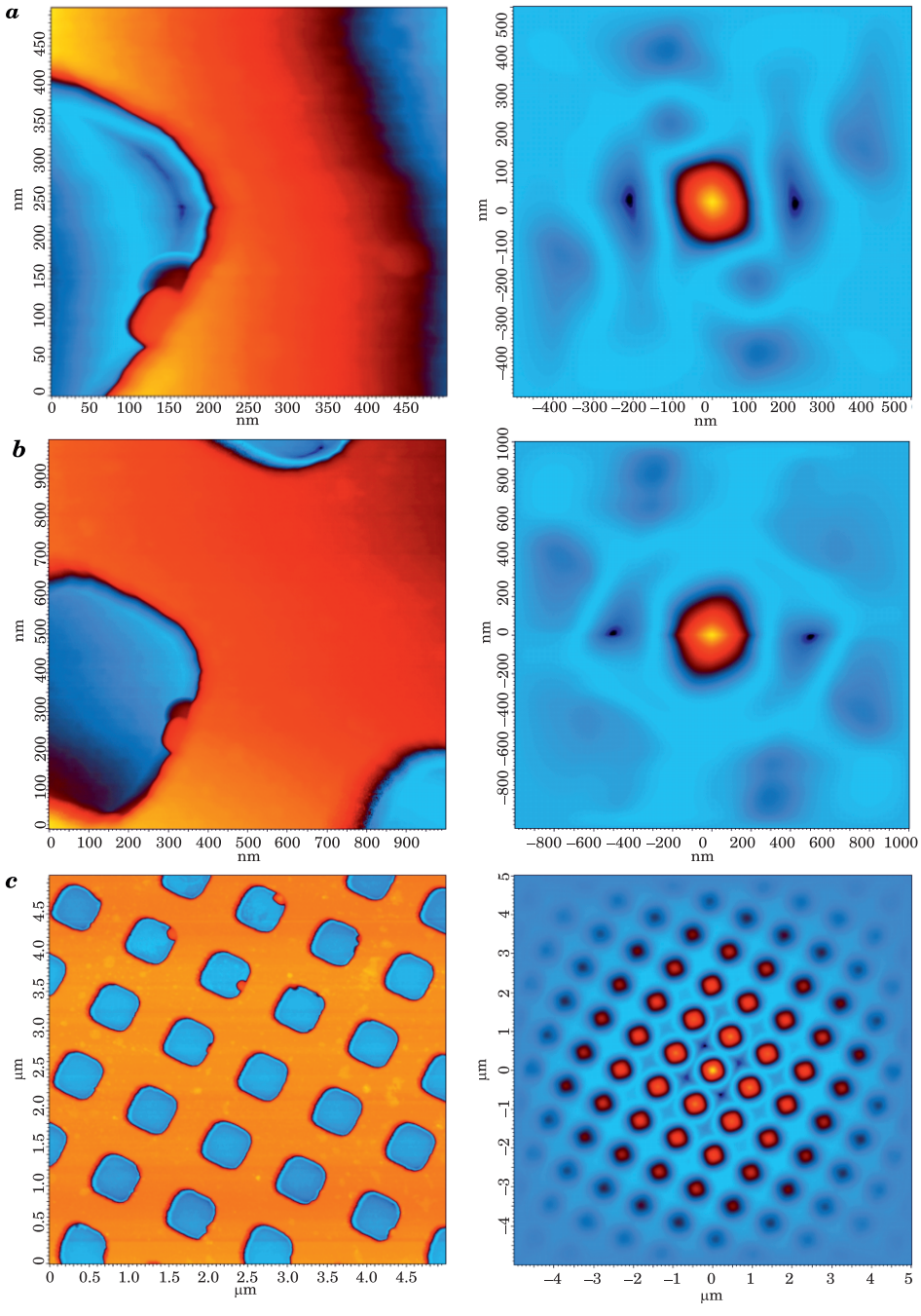

Fig. 4. Surface topography (left) and the spectra of the surface autocorrelation function (right) of the reference PG sample in the tapping mode. Scan size, respectively: *a* – 0,5×0,5 μm, *b* – 1×1 μm, *c* – 5×5 μm. Note the surface inhomogeneities seen in the topography images

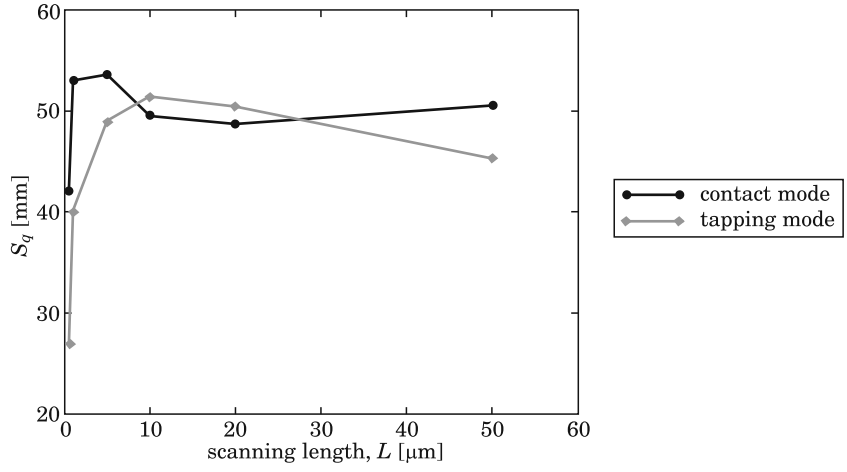

Fig. 5. Changes in root-mean-square roughness S_q as a function of the scan size in contact mode (circles) and tapping mode (squares)

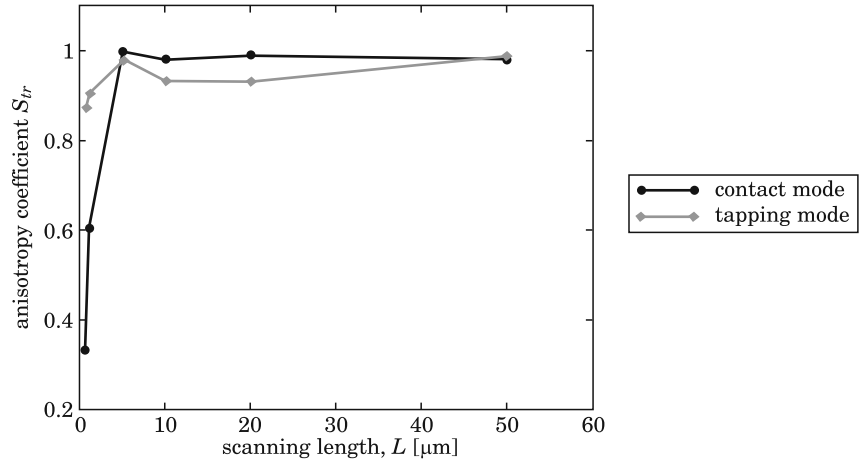

Fig. 6. Plot of the anisotropy coefficient S_{tr} as a function of the scan size in contact mode (circles) and tapping mode (squares)

Plots of the structure function $S(\tau)$ defined according to Eq. (4) for the scan size larger than 5 μm are shown in Fig. 7 and Fig. 8. Each plot is drawn for the scan directions parallel to the coordinate axes (x and y, respectively).

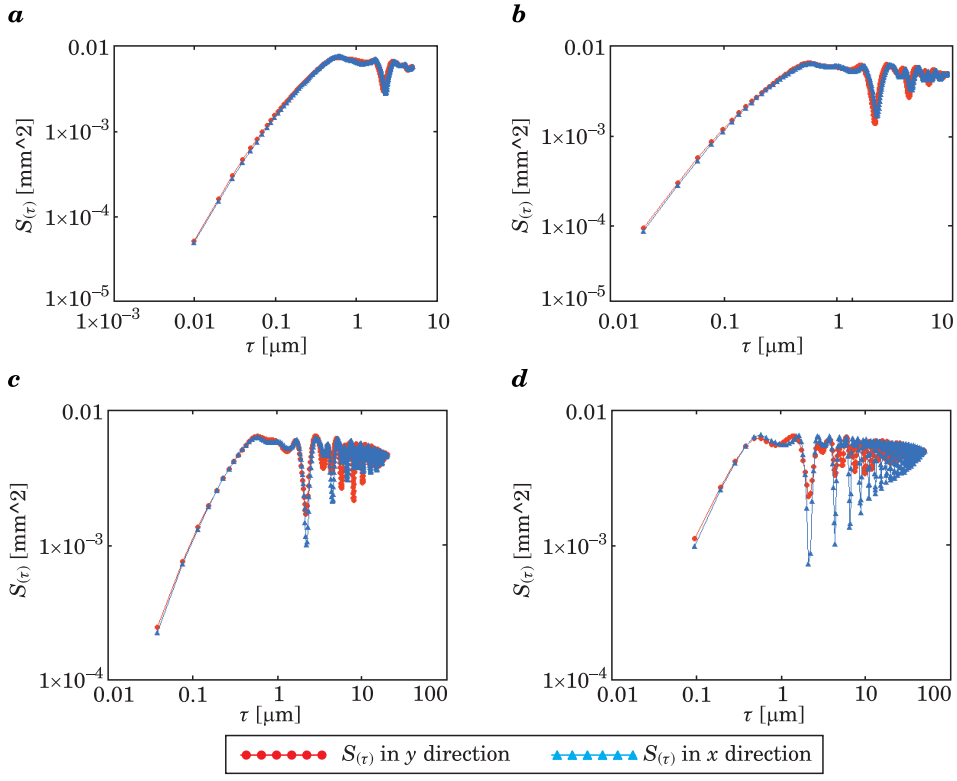

Fig. 7. Structure function $S(\tau)$ in contact mode for the scan size: *a* – 5×5 μm, *b* – 10×10 μm, *c* – 20×20 μm, *d* – 50×50 μm

Plots of the structure function shown in Figure 7 and Figure 8 are very similar independent of the scan direction, including the slope (corresponding to fractal dimension D), and the vertical intercept (corresponding to the topothesis K). As a rule, the fractal parameters of the isotropic surfaces become constant in any direction. For smaller scans, however, plots of the structure function $S(\tau)$ have different slopes depending on the scan direction.

In order to determine the fractal parameters of the sample surface assuming its self-affinity, log-log plots of the structure function $S(\tau)$ were drawn in Figure 9 for the scan size of 5, 10, 20 and 50 μm. Pronounced and reproducible linear range of each curve was approximated by the straight line, slope of which was twice as large as the Hurst parameter H ($a = 2H$), which subsequently allowed for determination of the fractal dimension D ($D = 2 - H$). As seen in Figure 9, estimated fractal parameters have similar values, especially the topothesis K. Additionally, the linear parts of the $S(\tau)$ curves in the tapping mode almost perfectly overlap, while in the contact mode a small

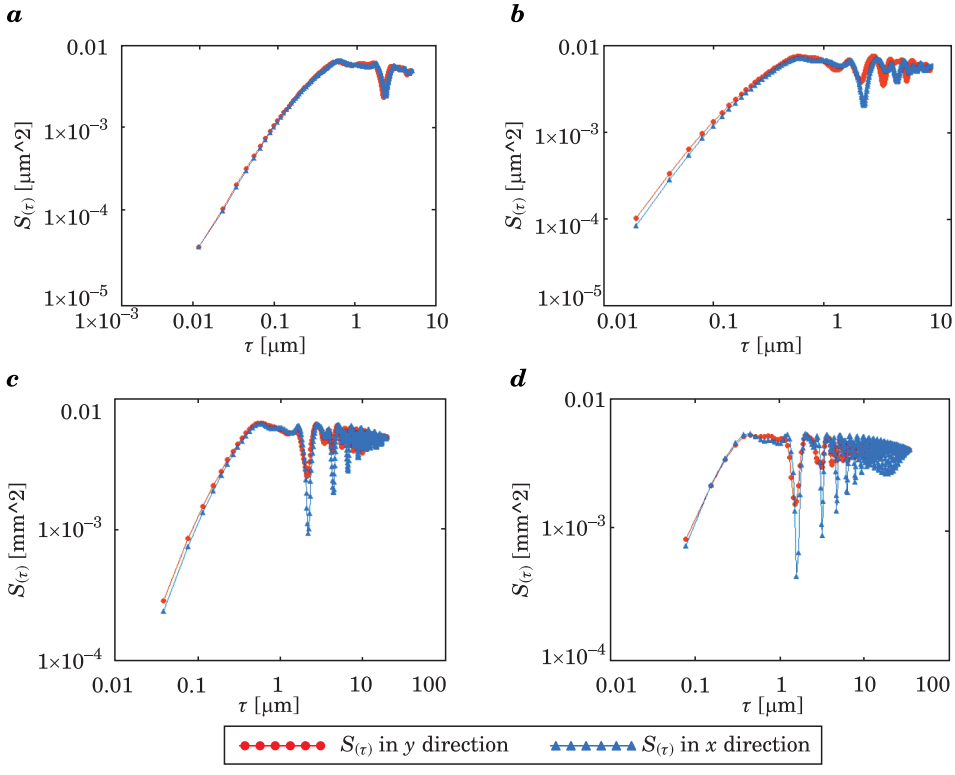

Fig. 8. Structure function $S(\tau)$ in tapping mode for the scan size: *a* – 5×5 μm, *b* – 10×10 μm, *c* – 20×20 μm, *d* – 50×50 μm

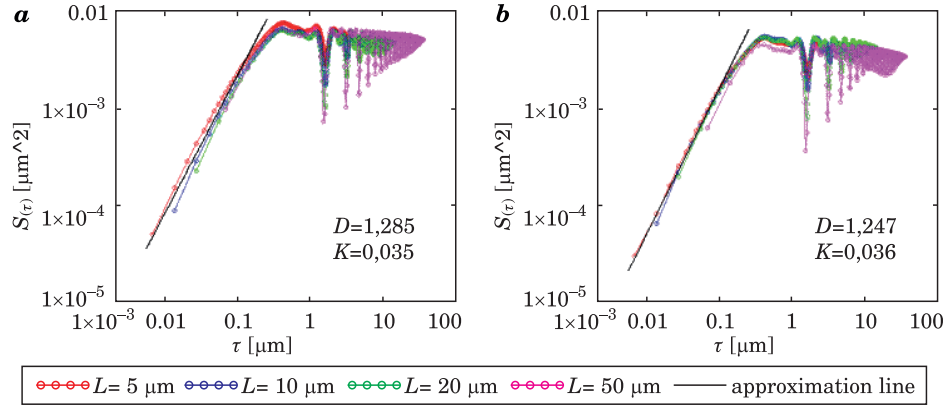

Fig. 9. Results of the straight line fit to the linear range of the structure functions and estimated fractal parameters obtained for isotropic images in: *a* – contact, *b* – tapping modes

deviation from the main direction can be observed that gives rise to a small deviation in the fractal dimension D.

AFM measurements do not exhibit the real surface topography. In fact, the AFM images are distorted by the tip shape and hence they provide the convolution of two curves, namely the surface and the tip curvature. However, all the measurements described in the paper were carried out using identical AFM probes, so that a comparison between contact and tapping modes is still possible. Figure 10 shows examples of scanning profiles (surface sections) recorded in both modes, which look very similar. This leads to conclusion that

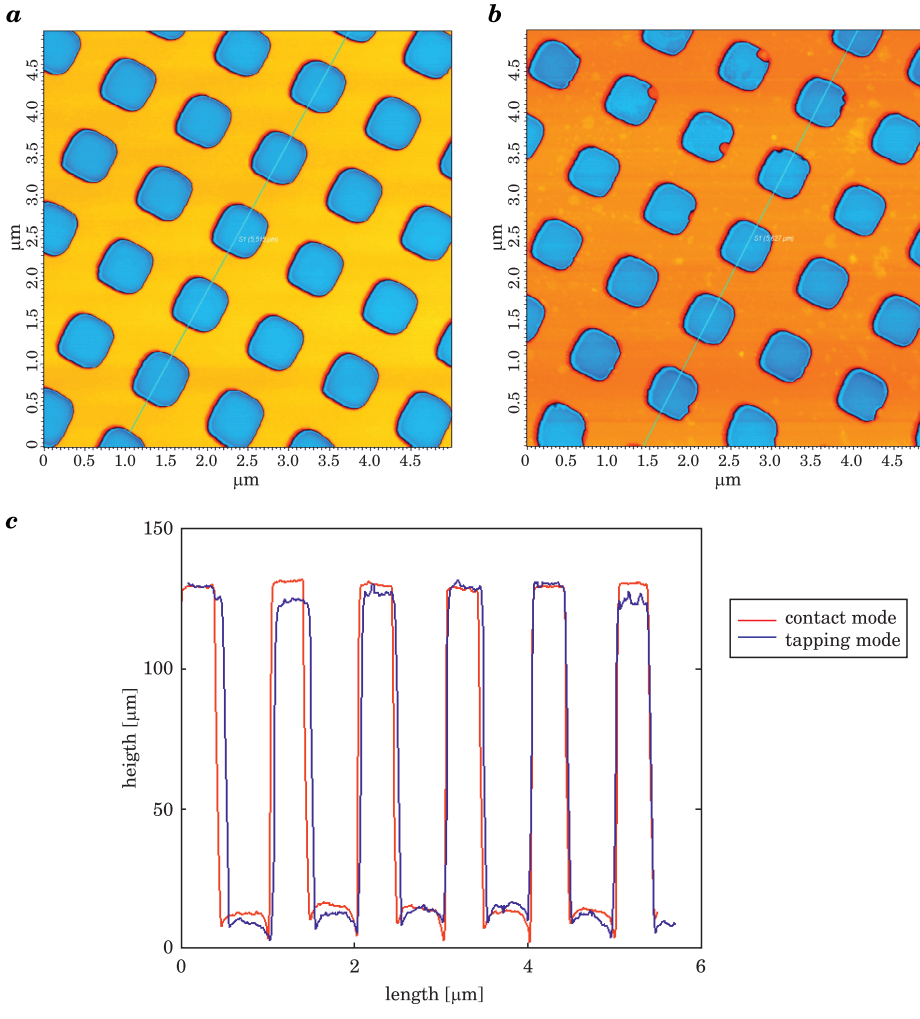

Fig. 10. Section profiles of the surface in: contact (red) and tapping (blue) modes

the differences in surface topography observed in contact and tapping modes are mainly due to the scanning method, and more specifically – the smallest distance between the tip and the surface.

Conclusions

A comparison between AFM measurements of the surface topography in contact and tapping modes reveals that in the multifractal domain, that is when at least one periodic element of the topography appears in the image, anisotropy coefficient S_{tr} can be assessed on AFM results obtained using either contact or tapping mode. The same applies to fractal parameters, although with small differences in the fractal dimension D. Note, however, that recorded images are results of many various tip-surface interactions, and hence getting the real surface topography in meso- as well as microscale requires deconvolution to be made prior fractal analysis.

Translated by Sławomir Kulesza

Accepted for print 16.11.2012

References

Bramowicz M., Klysz S. 2007. *Application of Atomic Force Microscopy (AFM) in the diagnosing of a surface layer*. Research Works of AFIT, 22: 167–174.

Bramowicz M. 2009. *Zastosowanie mikroskopii sił atomowych (AFM) w ocenie stopnia anizotropii mikrostruktury*. Inżynieria Materiałowa, 4: 235–238.

Hartmann U. 1997. *An Elementary Introduction to Atomic Force Microscopy and Related Methods*. Institute of Experimental Physics, University of Saarbrucken, D-66041 Saarbrucken, Germany.

Howland R., Benatar L. 2002. *STM/AFM Mikroskopy ze skanującą sondą elementy teorii i praktyki*. Tłum. M. Woźniak, J.A. Kozubowski (WIM PW), Warszawa.

Mainsah E., Greenwood J.A., Chetwynd D.G. 2001. *Metrology and Properties of Engineering Surfaces*. Kluwer Academic Publishers.

Mironov V.L. 2004. *Fundamentals of Scanning Probe Microscopy*, The Russian Academy of Sciences. Institute of Physics of Microstructures, Nizhniy Novgorod.

Saint Jean M., Hudlet S., Guthmann C., Berger J. 1999. *Van der Waals and capacitive forces in atomic force microscopies*. J. Appl. Phys., 86(9): 5245–5248.

PN-EN ISO 25178-6:2011 – Specyfikacje geometrii wyrobów (GPS). Struktura geometryczna powierzchni: Przestrzenna.